Chapter 2: Site characteristics

Authors: L. Valenziano, V. Minier, P. Tremblin, G. Durand, M. De Petris, S. De Gregori, L. Lamagna, J. Pardo, L. Sabbatini, N. Schneider, (others to be included)

2.1 Introduction

The main goals are to summarise the current knowledge of Dome C in terms of atmospheric transmission, frost formation, thermal gradients and turbulences, and phase stability for interferometry; it will be based on meteorological data and PWV derivation, direct measurement and modelling of the transmission, current understanding of turbulence and thermal gradients in the 45-m layer above ground. Future site testing experiments will be proposed. Transmission in the 200, 350 and 450 μm bands should be measured/estimated. Comparisons with Chajnantor sites (up to 5800 m) and South Pole.

Site testing in the sub-millimetric range can be performed with many complementary methods. Relevant quantities to be evaluated are Atmospheric transmission (Opacity) in the astrophysical interesting bands, atmospheric stability (turbulence), wind speed (for mechanical effects on large antennas). This quantities can either be evaluated from:

1. indirect measurements meteorological data (meteo stations, radiosoundings), instruments for atmospheric studies (spectral hygrometer, solar irradiance, SODAR)
2. Direct measurements (sub-millimiter spectrometers, tipper)

Site testing activities started at DomeC in 1995, when the first scientific team launched balloons and measured the sky noise in the millimetric wavelength range.

2.2 Indirect meteorological data: Ground based data

Meteorological parameter at Dome C are available via Automatic Weather Stations (AWS) (a project run at the University of Wisconsin, Madison and funded by the National Science Foundation of the Unites States of America) and by some on-site dedicated instruments.

2.2.1 Wind speed

Wind speed regime at DomeC is extremely low, as it is reported in Valenziano & Dall'Oglio, 1999, Lawrence, 2004 and Aristidi et al., 2005. Average values over the whole year is between 2.4 and 3.0 m/s, compared with a value of between 5.5 and 6.3 m/s at the South Pole. This is due to the geographical location on a dome, where katabatic winds are less intense.

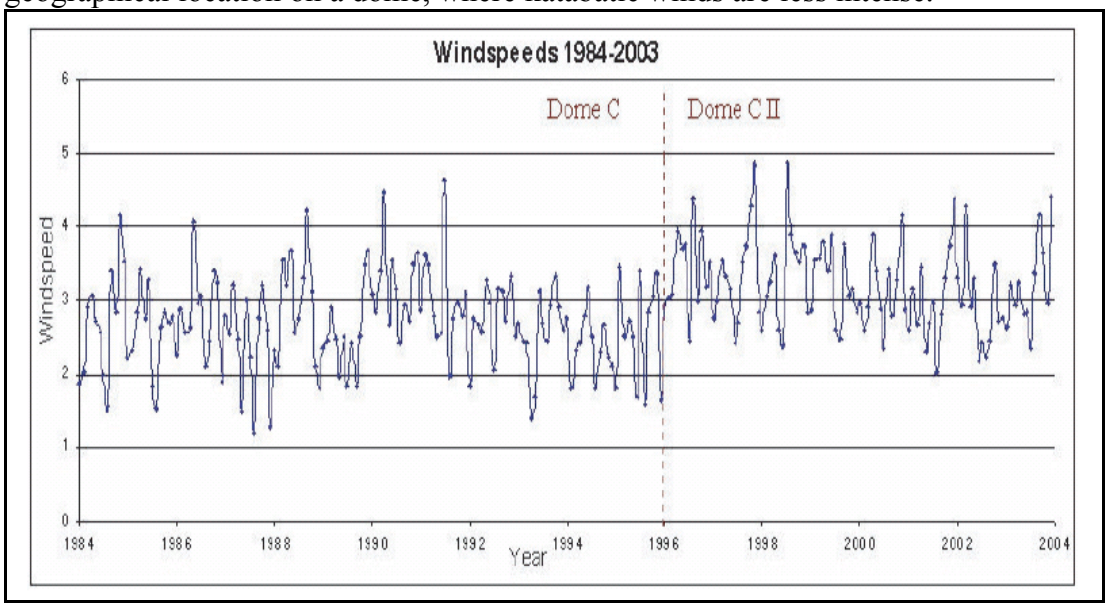

Figure 1: Wind speed measured at DomeC over 20 years (from Aristidi et al., 2005)

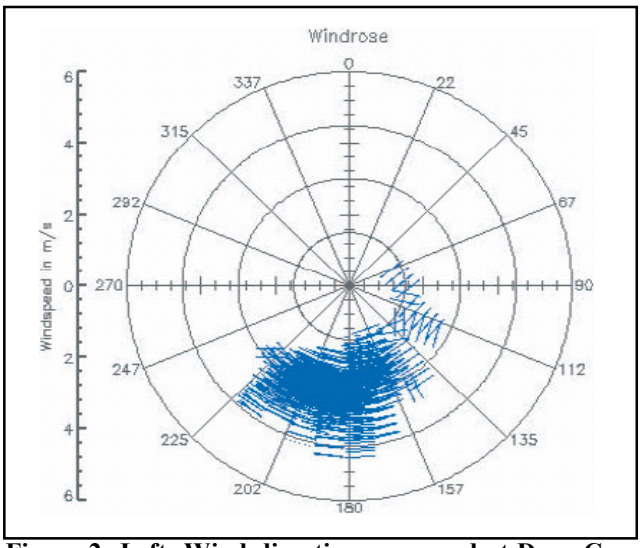

Figure 2: Left: Wind direction measured at DomeC over 20 years (from Aristidi et al., 2005). Right: The same, measured in summer 1997. (From Geogiadis et al., 2002).

Site	Average Wind Speed	Reference
AWS - Dome C (1984 – 1995)	2.7	Aristidi et al., 2005
AWS – Dome C II (1996 – 2003)	3.2	Aristidi et al., 2005
DomeC + DomeC II	2.9	Aristidi et al., 2005
Mauna Loa	4.4	Barnes, 2004
La Silla	4.6	Hainaut, 2004
South Pole	5.5	Mefford, 2004
Paranal	6.6	Hainaut, 2004

Comparison of average wind speed measured at submillimetric astronomical sites. Adapted from Aristidi et al., 2005

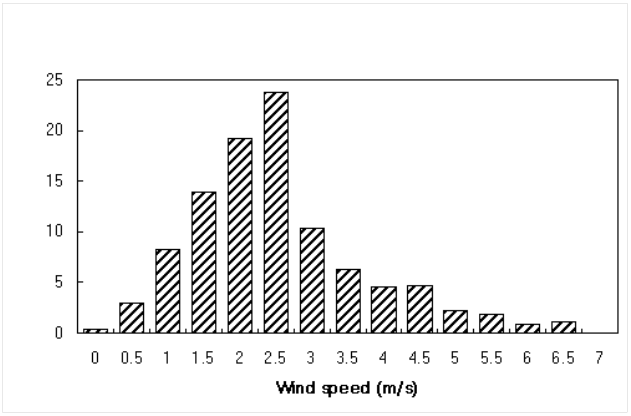

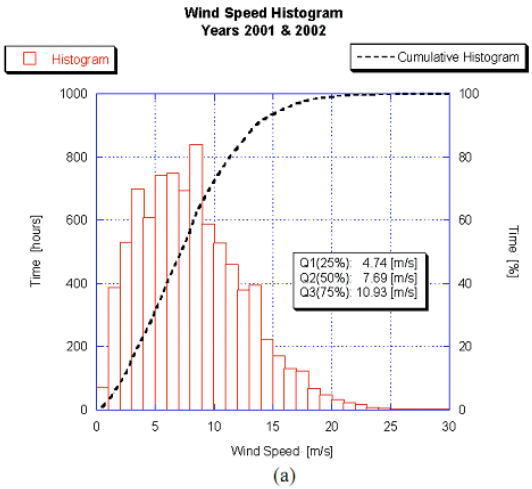

Figure 3: Left: Wind speed distribution at DomeC in summer 1997 (From Geogiadis et al., 2002). Right wind speed distribution at Chajnantor (from Beaupuits et al., 2004).

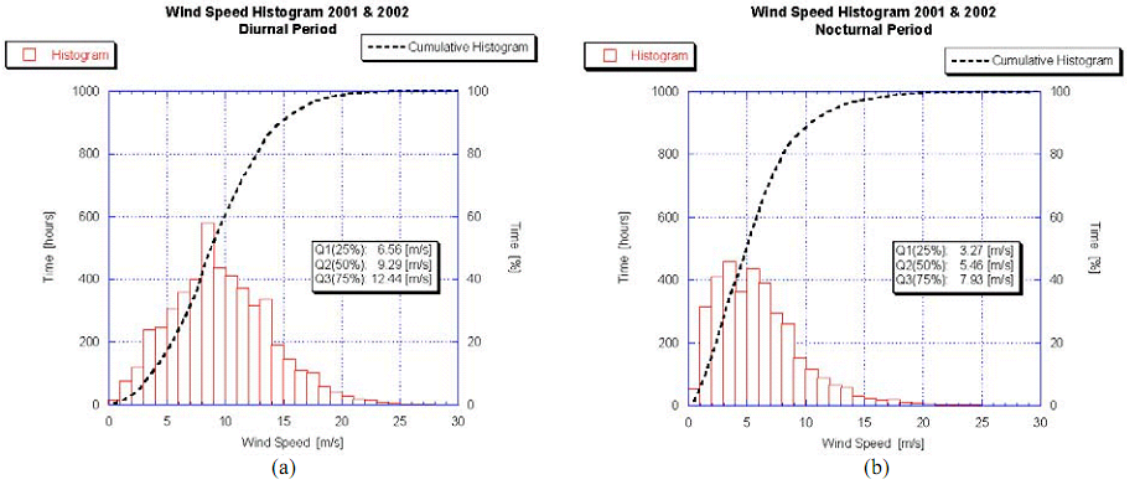

Figure 4.2 (a) and (b) Wind speed histogram of the diurnal and nocturnal periods, respectively, for 2001 and 2002 together.

Figure 4: Wind speed at Chajnantor (from Beaupuits et al., 2004). Note that even at nighttimes wind speed is significantly higher than at Dome C.

2.2.2 Temperature

The average ground temperature at DomeC is ranging between -65°C in winter and -26°C in summer. Two peculiar characteristics are present in the data:

- a diurnal temperature oscillation of about 12°C during summer months. This fact is less evident at South Pole and it is mostly due to the effect of Sun irradiance.
- a quasi-periodic large (up to 30 °C variation in a week) ground temperature oscillation during the winter. An example is reported in Figure 5.

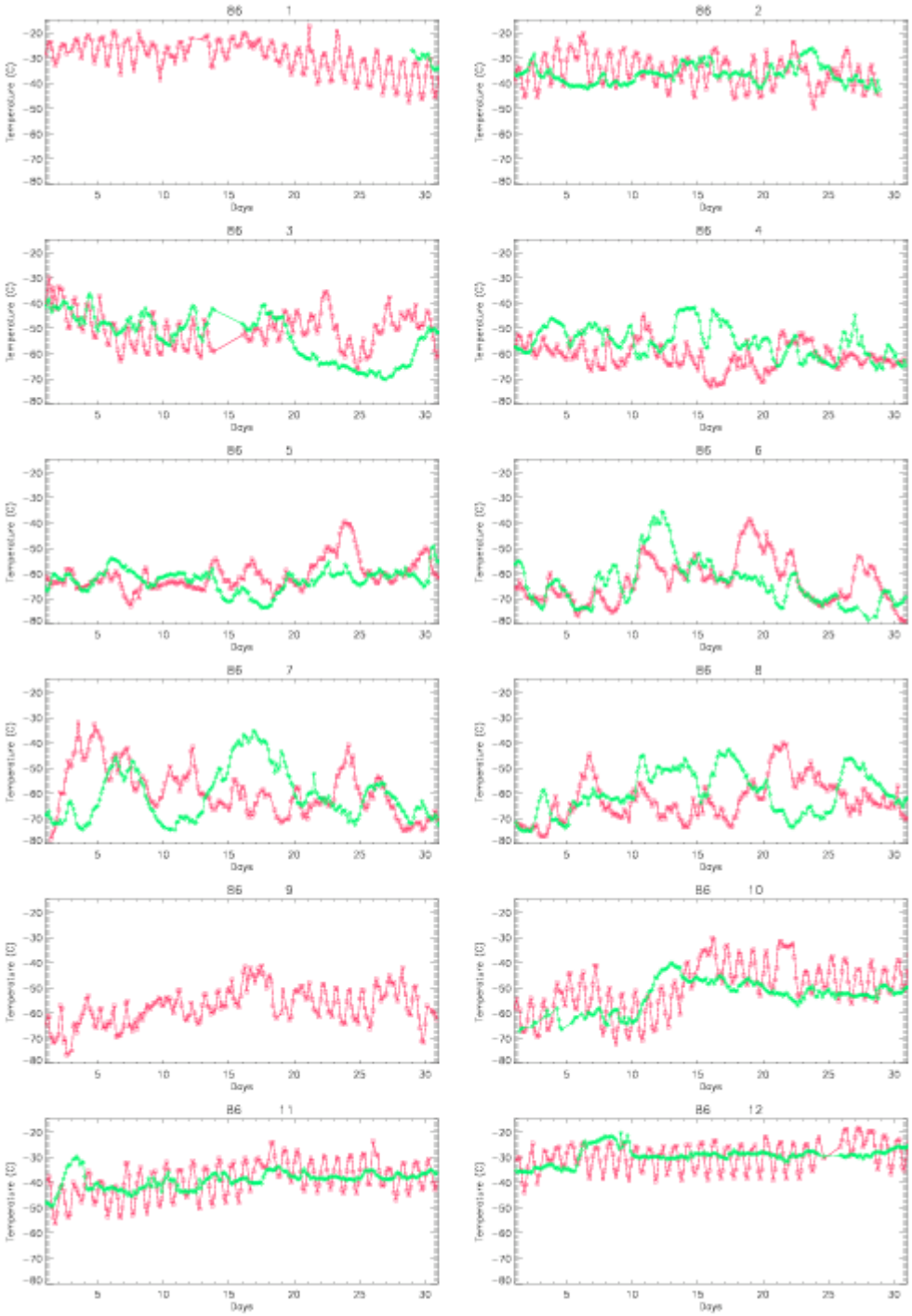

Figure 5: Ground temperature data measured by AWS in 1988 at DomeC (red) and South Pole (green) (from Valenziano, 2005). Diurnal cycle at DomeC is evident during summer, from late September throughout March. Note the large temperature oscillation in winter.

2.2.3 Pressure

Data from radiosoundings (see next section) yield the following mean monthly values of the surface-level pressure: p_o = 658.0 ± 5.1 hPa in December, p_o = 650.7 ± 3.6 hPa in January, p_o = 640.1 ± 1.6 hPa in March, p_o = 635.1 ± 5.2 hPa in April, and p_o = 641.0 ± 6.7 hPa in May. These results agree satisfactorily with the yearly median value of 644 hPa found by Valenziano and Dall'Oglio (1999) at Dome C, examining the Automatic Weather Station (AWS) meteorological data recorded from 1986 to 1993. This level corresponds to a barometric elevation of about 3700 m at mid-latitudes.

2.3 Radiosoundings

Radiosoundings are a powerful tool to analyze meteorological data and to derive quantities relevant to astrophysical site testing. Balloon sondes are routinely launched at DomeC by meteorologist group of the Antarctic Project (ENEA, C. R. Casaccia, Rome, see www.climantartide.it for details). This activity was started in 2005 having the purpose of implementing the radiosounding station facility, satisfying the SCAR recommendation SCAR XXVII-12 to provide "upper air data on the Antarctic Plateau, in order to both improve numerical atmospheric modelling and precipitable water estimates and test novel vertical profiling techniques, such as GPS and other remotely sensed profiling".
A first data set was acquired by the group of the University of Nice (France) and consisting of 101 radiosoundings taken in December 2003 and January 2004 (Aristidi et al., 2005).

2.3.1 Correction for systematic effects

As reported in the literature, radiosonde sensors are affected by systematic (Miloshevic et al., 2004, 2006, Wang et al., 2002), which must be corrected to obtain reliable data. A procedure, described in Tomasi et al. 2006 and briefly outlined below, was applied to radiosoundings to obtain reliable data.

Two type of sondes by Vaisala have been used: RS80-A and RS92. Radiosondes data, acquired in Antarctic temperature and humidity conditions, are affected by some systematic effects, each one considered and corrected in the procedure (see Tomasi et al., 2006 and references therein): (1) Environmental effects on thermocap sensor, such as solar irradiance, heat conduction through attachment points, radiation emitted from the sensor itself, (2) lag errors on temperature data, mainly due to pressure change and ventilation effects, (3) errors on RH data due to the Humicap sensor, such as temperature dependence, chemical contamination, basic calibration model. These effects are dependent on the radiosonde model used, being less important for the RS92 one, the most frequent in this second dataset. Data reduction was carried out following the procedure fully described in Tomasi 2006. We report here the main significant steps applied. Temperature data from RS80 thermocap sensors were corrected according to *Tomasi et al.* [2004]. Lag errors from RS92 sensors were neglected according to *Luers* [1997]. The RH data from RS80 were corrected according to *Miloshevich et al.* [2004], by applying the same procedure as for the first dataset. Correction for the RS92 were neglected,according to *Miloshevich et al.* [2006]. Correction for RH lag errors was applied to all data.

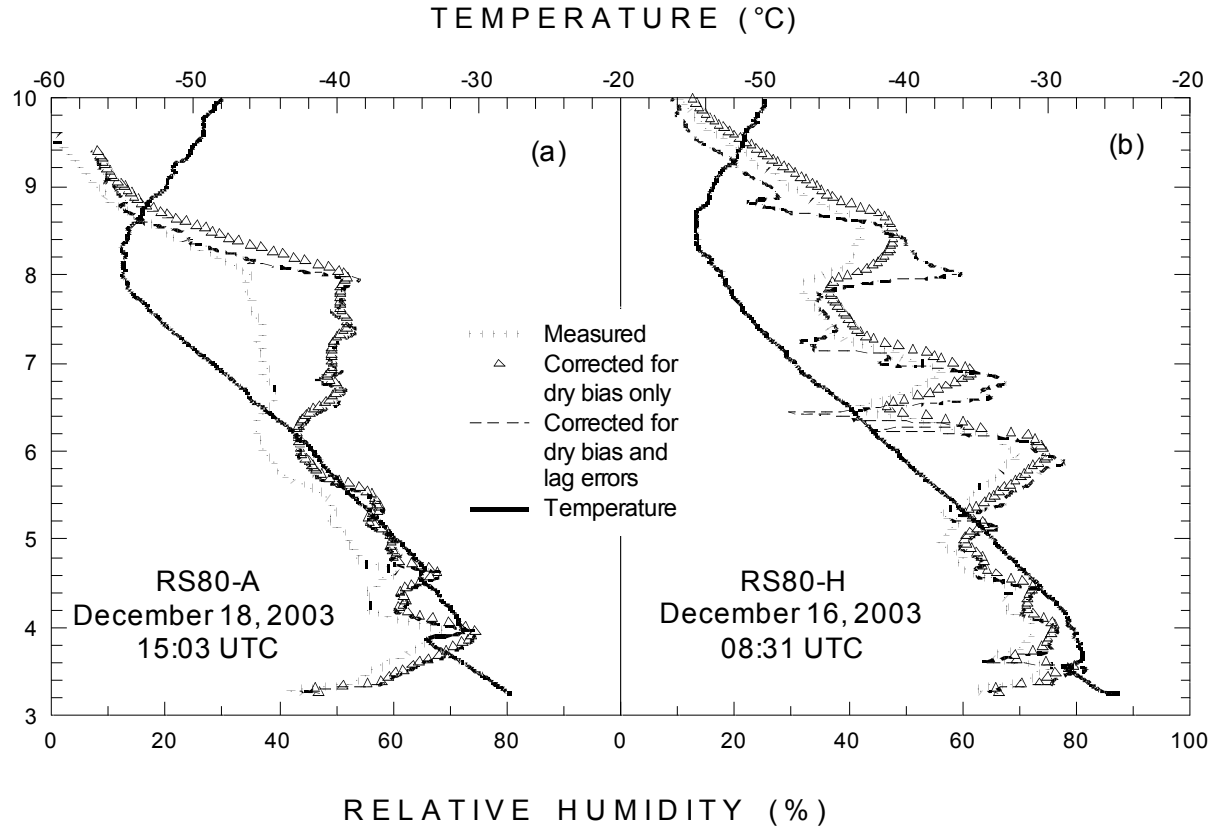

Figure 6: Vertical profiles of air temperature (solid curves) and relative humidity RH obtained from the radiosounding data taken on December 18, 2003 (15:03 UTC) using a RS80-A radiosonde (on the left) and on December 16, 2003 (08:31 UTC) using a RS80-H radiosonde (on the right). The original RH data provided by the radiosondes are given by small solid circles (From Tomasi et al., 2006).

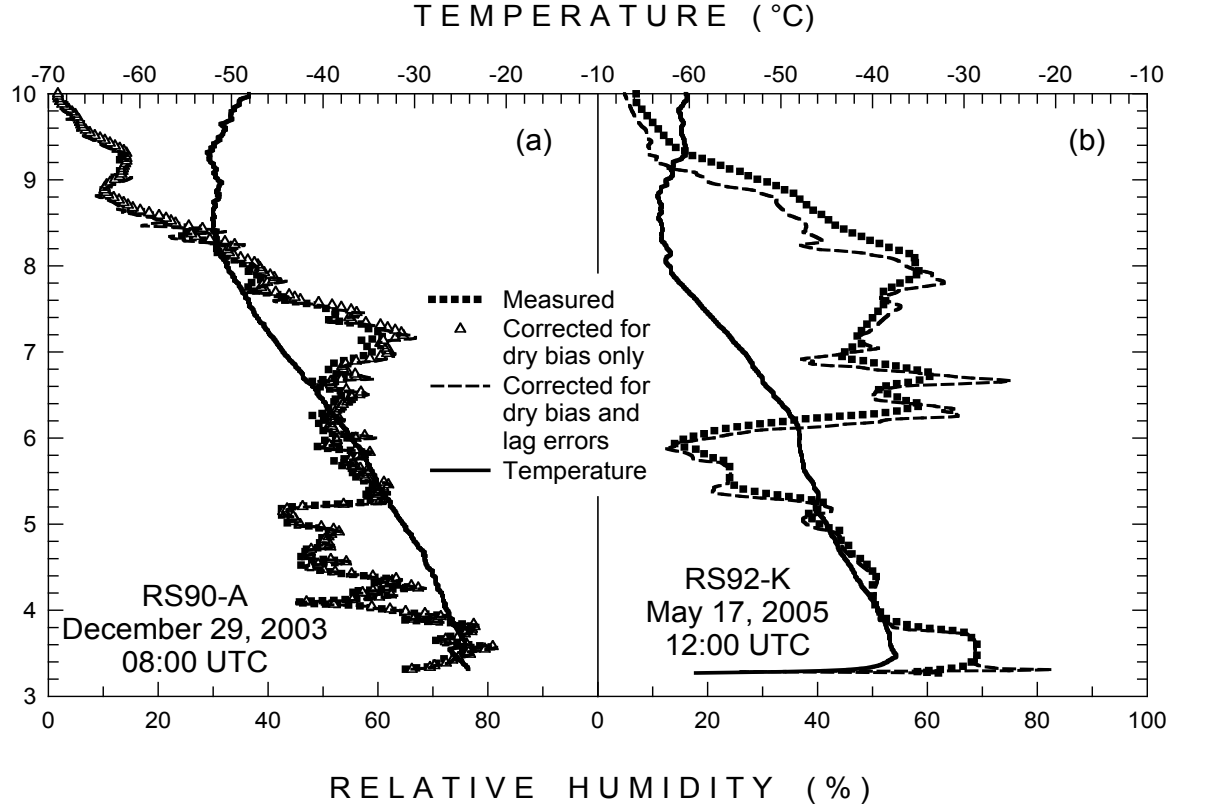

Figure 7: As in Figure 6, for the RS90-A radiosounding data taken on December 29, 2003 (08:00 UTC) (on the left) and for the RS92-K radiosounding data taken on May 17, 2005 (12:00 UTC) (on the right). The right part shows only the vertical profiles of the original RH data (small solid circles) and the time-lag corrected and smoothed RH data, since the RS92-K RH measurements do not need to be corrected for the dry bias.

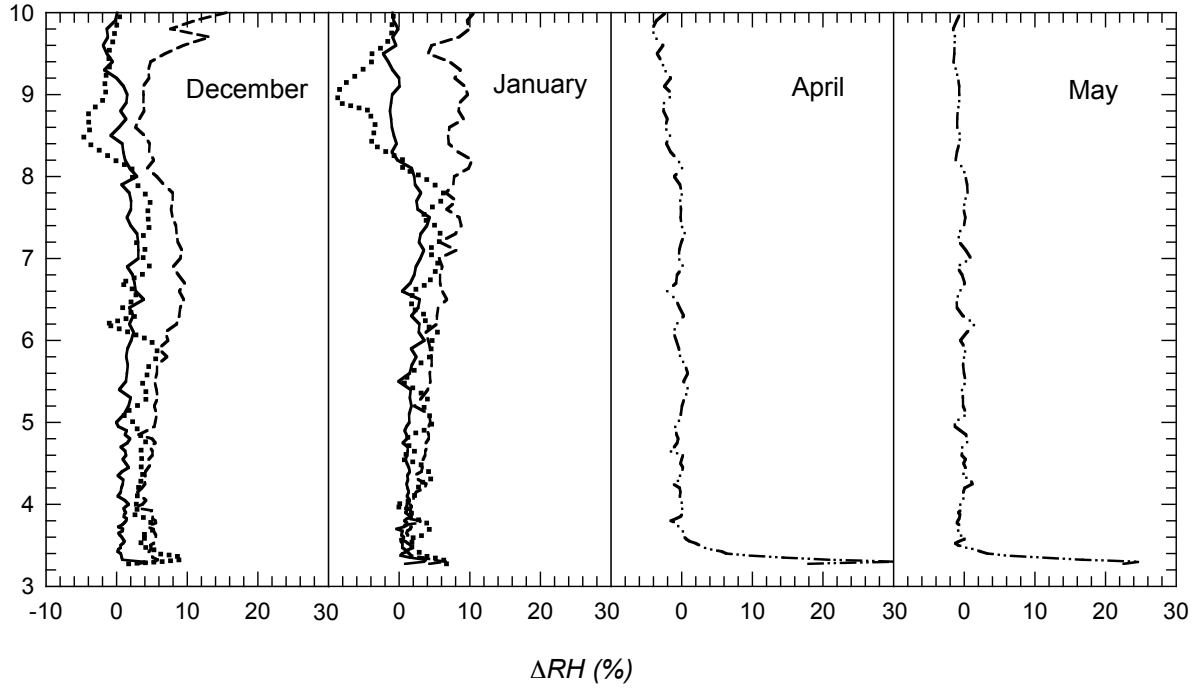

Figure 8: Mean monthly vertical profiles of parameter *ΔRH* given at each level by the sum of the dry bias and lag errors determined following the W02 and M04 procedures adopted in Section 2, for the monthly *RH* data-sets of December, January, April and May. Dashed curves refer to the RS80-A data, dotted curves to the RS80-H data, solid curves to the RS90-A data, and dashed and dotted curves to the RS92-K data.

A first data set is analysed in Tomasi et al., 2006. It consists of two sub-sets carried out in different months by two research groups currently working at this Antarctic station: (i) a first sub-set provided by the group of the University of Nice (France) and consisting of 101 radiosoundings taken in January 2003, December 2003, and January 2004 (Aristidi et al., 2005), and (ii) a second sub-set consisting of 37 radiosoundings only, taken by the meteorological group of the Antarctic Project (ENEA, C. R. Casaccia, Rome) during March, April and May 2005.

Each radiosounding measurement provides the values of the various thermodynamic parameters at numerous significant levels. In general, more than 600 significant levels were found in the troposphere, usually taken every a few meters one from the next, and more than 1700 were found in the stratosphere.The thermodynamic parameters given directly by the radiosondes were the following: (i) time τ after the launch, measured with the precision of 1 s, (ii) geometrical altitude Z (in m), (iii) pressure p (in hPa), (iv) air temperature T (in °C), and (v) relative humidity RH (in %). The ascent rate v of the radiosonde (m s^{-1}) was subsequently calculated from the sequence of pairs of values of τ and Z determined at each significant level.

2.3.2 Temperature profiles

We report here some results from Tomasi et al. (2006). For each vertical profile of T obtained from the various radiosounding monthly data-sets, the values of T at the first significant value given by the radiosonde (usually ranging between 3265 and 3270 m heights) are calculated, along with 172 fixed levels from 3275 m height to the 25 km level. All the data defining 138 vertical profiles of T were then subdivided into five monthly sets, for which the average monthly values of T were calculated at all the fixed levels together with the corresponding standard deviations. The vertical profiles thus obtained are shown in Fig. XX. As can be seen, the troposheric region is subject to a

strong cooling, passing from the austral summer months (December and January) to the fall ones (March, April and May), by about 10 °K on the average throughout the whole troposphere and by more than 25 °K at the ground. The temperature minimum characterizing the tropopause region appears to become more pronounced in March and April, since the cooling processes affecting the lower part of the stratosphere are limited in these months within the narrow layer having depth of a few kilometres above the tropopause level. On the contrary, the cooling of the stratosphere is more marked in May, the temperature decreasing further by more than 10 °K throughout the stratosphere, above 9 km height.

Figure XX also shows that the mean monthly temperature values at the surface-level are around 245 °K in December and January and around 220 °K from March to May, these findings being in accordance with the results found by Valenziano and Dall'Oglio (1999) at Dome C over a 7-year data-set of AWS meteorological data, from which average seasonal values of ground-temperature equal to –65 °C (~ 208 °K) in the austral winter and –26 °C (~ 247 °K) in summer were found, with an annual median value of –53 °C (~ 220 °K). The results for surface temperature in Tomasi et al., (2006) are therefore fully comparable with the findings of Valenziano and Dall'Oglio (1999) and those reported by Aristidi et al. (2005).

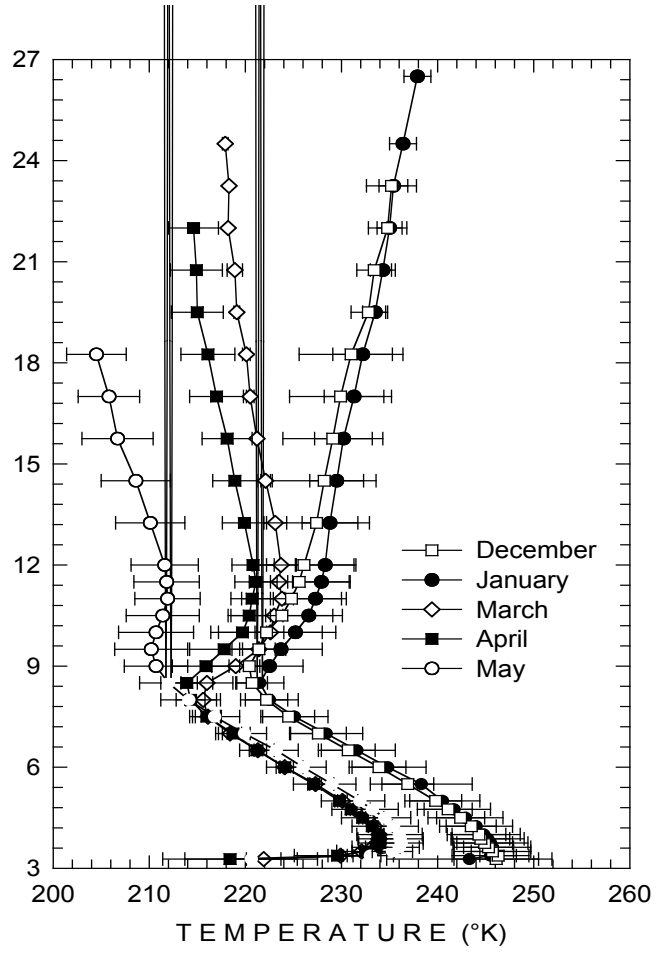

Figure 9: Mean monthly vertical profiles of air temperature *T* (°K) obtained from the monthly data-sets relative to December (open squares), January (solid circles), March (open diamonds), April (solid squares) and May (open circles). The bars represent the standard deviations obtained at some significant fixed levels, giving a measure of the dispersion of the monthly data. (From Tomasi et al., 2006)

2.3.3 Humidity profiles

We report here some results from Tomasi et al. (2006).

The overall set consisting of 138 vertical profiles of parameter q was then subdivided into five monthly sub-sets to determine the mean monthly values of this parameter at the first significant level and the other 172 fixed levels from 3.275 to 25 km, together with the corresponding standard deviations. The results are shown in Figure 10, giving evidence of the marked variations in the moisture conditions of the troposphere taking place at all levels from the surface up to 8 km altitude, when passing from the December/January period to the austral fall months. These large changes indicate also that precipitable water is expected to assume values in the austral fall months that are considerably lower than those observed during the austral summer.

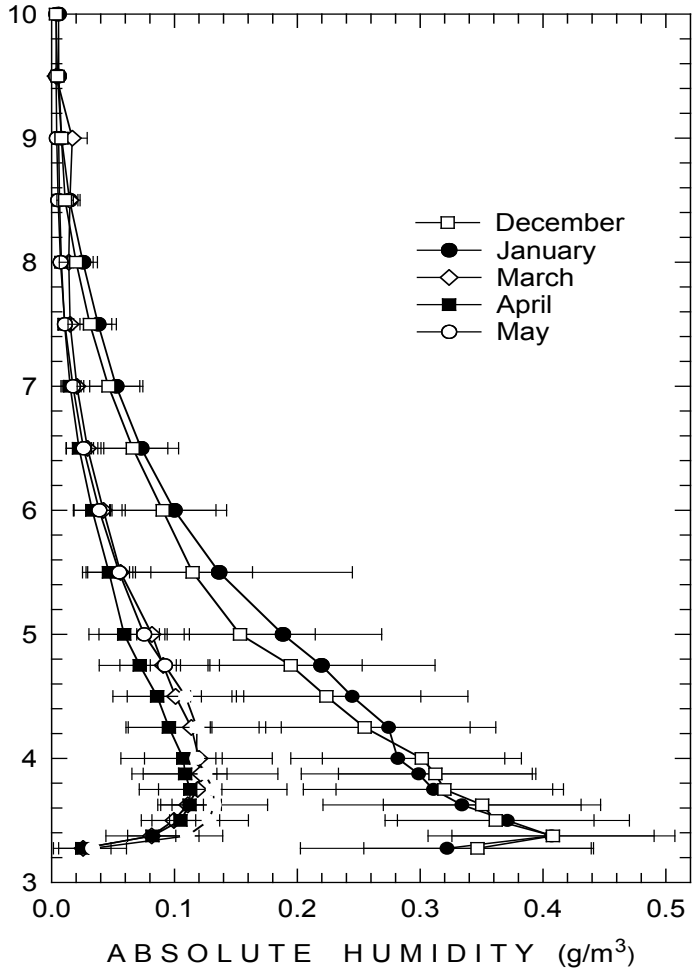

Figure 10: Mean monthly vertical profiles of absolute humidity *q* (g m^{-3}) obtained from the monthly data-sets of *q* relative to December (open squares), January (solid circles), March (open diamonds), April (solid squares) and May (open circles). The bars represent the standard deviations obtained at some significant fixed levels, giving a measure of the dispersion of the monthly data.

2.4 PWV content

2.4.1 PWV from radiosounding

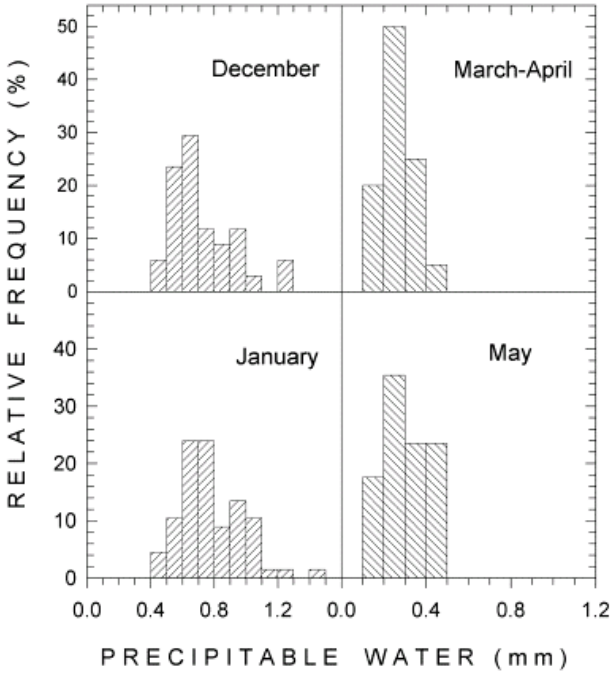

Figure 11: Precipitable Water Vapor content evaluated from the first set of radiosoundings.

Data from radiosoundings can be used to derive PWV content for all the the 138 vertical profiles of q determined in Tomasi et al. (2006), by integrating the absolute humidity from the surface-level up to the top-level measured by the Humicap sensor, and then adding the precipitable water contribution given by the atmospheric region between the Humicap sensor top-level and the 10 km height, as calculated through integration of the mean monthly vertical profiles of q presented in Figure 10, in all cases where such a calculation needs to be completed. These evaluations of W were then subdivided into four monthly sub-sets, relative to the December, January, late March/April (hence, including also the 4 days from March 25 to 30), and May periods, respectively. For these sub-sets, the following mean monthly values were obtained together with the corresponding standard deviations: $W = 0.72 \pm 0.20$ mm STP in December, $W = 0.76 \pm 0.19$ mm STP in January, $W = 0.26 \pm 0.08$ mm STP in March/April, and $W = 0.30 \pm 0.10$ mm STP in May. The results indicate that there is a limited increase of the mean monthly value of W from December to January and an appreciable increase from March/April to May. In order to better define the variations of W during the above monthly periods and the dispersion features of this atmospheric parameter, Figure 11 presents the relative frequency histograms of W drawn for the above four monthly sub-sets. The comparison between the December and January histograms indicates that the December data are characterized by bimodal features centered at about 0.65 and 0.95 mm STP, respectively, whereas the January data give form to only one peaked distribution curve, which clearly appears to be skewed to the right, throughout the range of W from 0.8 to 1.2 mm STP. Limited variations from December to January can be explained mainly in terms of episodic changes in the atmospheric humidity features rather than in terms of regular evolutionary patterns of the meteorological and thermodynamic features of the atmosphere from one month to the other. Therefore, the results shown in Figure 11 indicate that the moisture conditions of the troposphere observed above Dome C in December differ very little, on the average, from those measured in January.

Comparing in Figure 11 the relative frequency histograms obtained for the March/April and May sub-sets, it can be seen that precipitable water *W* measured on the last days of March and throughout April assumed very stable values.

Period			Precipitable Water Vapor (mm)	
		1st quartile	2nd quartile	3rd quartile
December		0.58	0.64	0.87
January		0.64	0.73	0.90
March/April		0.21	0.24	0.32
May		0.23	0.26	0.38

This results are in substantial agreement with direct measurements at DomeC in 1996-97 (Valenziano et al., 1998) using a portable sun photometer (Volz, 1983).

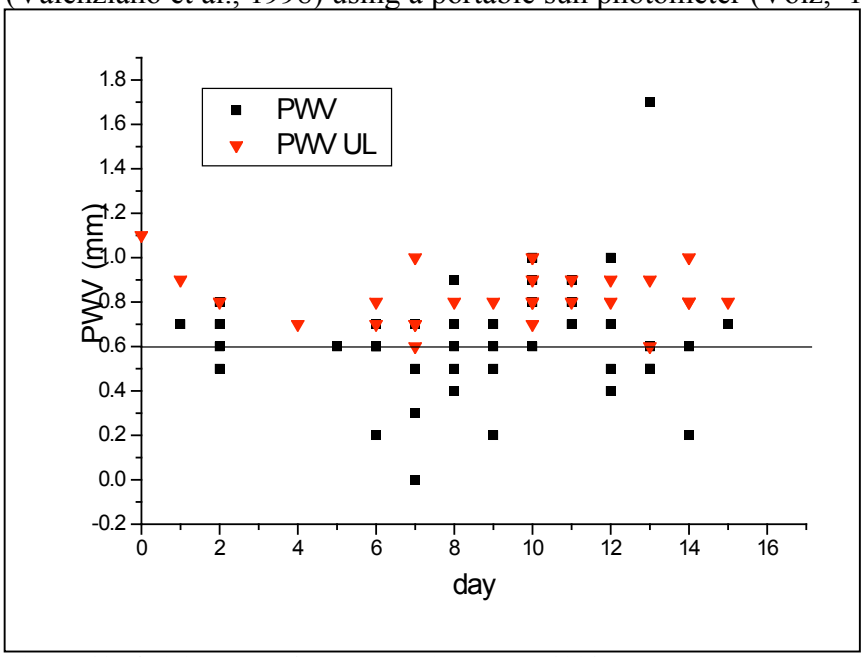

Figure 12: Original data from Valenziano et al, 1998.

These data have been further refined using a sophisticated calibration technique (Tomasi et al., 2008), yielding a better agreement with Tomasi et al., 2006.

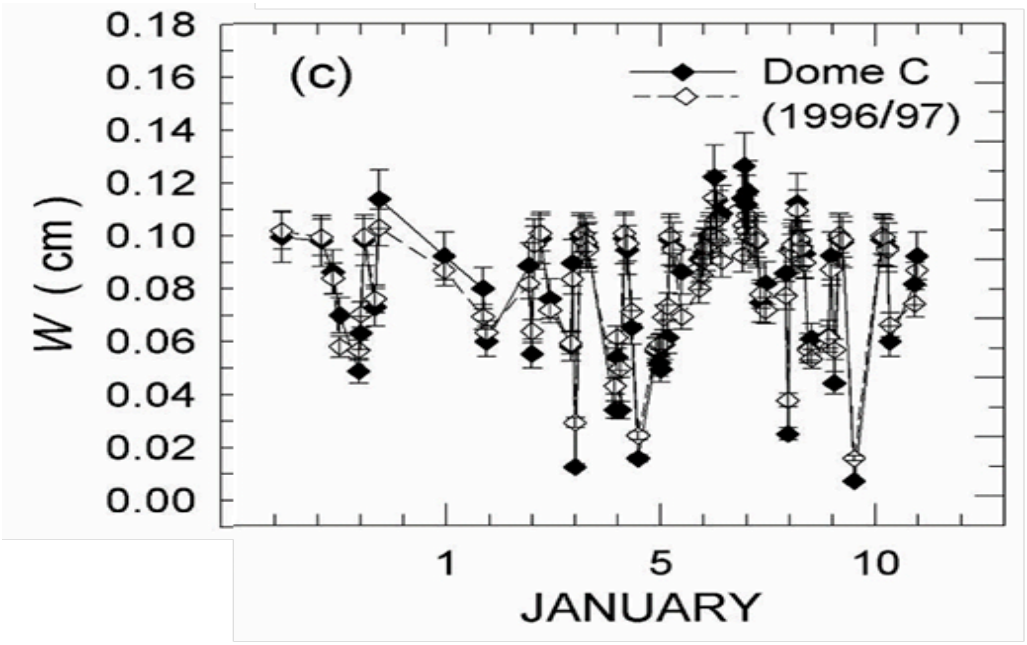

Figure 13: Refined calibration refined for DomeC 1996 PWV (from Tomasi et al,, 2008)

The analysis of a second radiosounding data-set is in progress (Valenziano et al, 2008), confirming the above findings. A preliminary plot of the obtained results, spanning over 1.5 years, is reported in the following plot.

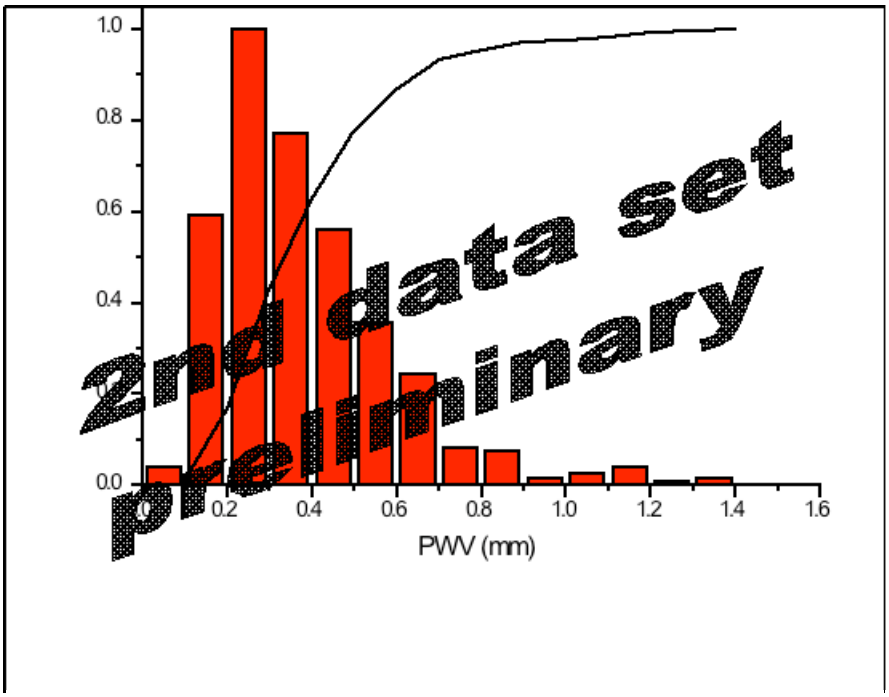

Figure 14: Preliminary data from the second data set of radiosoundings.

Data presented in this paper (see Table 2 for a comparison with other well-established sites) confirm that the high Antarctic Plateau is one of the driest site on Earth and it results in an exceptional transparency at infrared, sub-millimetric and millimetric wavelengths. When comparing the global site quality for astronomical observation between DomeC and South Pole, other parameters need to be considered. Dome C presents lower ground temperatures (i.e. lower telescope emissivity in the infrared), lower wind speeds and lower boundary layer turbulence, as illustrated in Valenziano and Dall'Oglio (1999), Lawrence (2004a - Nature), Lawrence (2004b – PASP). Moreover, observations in the far-infrared range (i.e. 40 – 300 □m) can only be performed on ground in exceptionally dry condition, which are episodically present on chilean (see Giovanelli et

al., 2001) sites but quite common in antarctic ones. A definitive comparison in terms of site quality for astronomy between South Pole and Dome C needs more data from the latter site. However, results in this paper and in the literature candidate DomeC to be superior in absolute terms. This advantage may represent a key point when projects for extremely large telescopes (diameter above 10m that cannot be carried on satellites) are concerned: even a small advantage in transparency or integration time may be a critical issue in site selection.

2.4.2 PWV from atmospheric transmission measurements

A major obstacle to carry out submm observations below 500 microns from ground is the atmosphere as well as the harsh environment of the potential Earth site (high altitude deserts; Antarctica). Preliminary meteorological studies and atmospheric transmission models tend to demonstrate that Dome C might offer atmosphere conditions that open the 200-µm windows. The SUMMIT submm tipper, a collaboration between CEA Saclay and UNSW/Sydney, has started operating in early 2008 for measuring sky opacity at 200 microns.

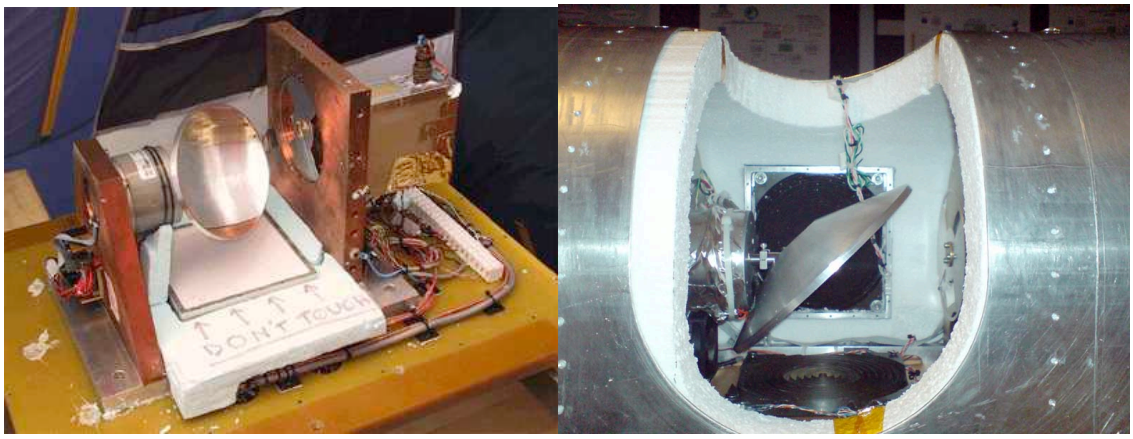

Figure 16: SUMMIT. Left: Inside with the mirror and the chopper wheel. Right: For 2008 campaign at Concordia the warm black body is kept warm in the airflow, heated by resistors. The reference black body at the rear is in contact with the cold aluminum cover.

Figure 17: SUMMIT in operations at Concordia with Cochise at the rear.

SUMMIT has been operating since March 2008 and works perfectly at Concordia. Data are available from the beginning of April until now, the preliminary results are given in figure 18. It was not possible to do a full calibration of the instrument before sending it at Dome C, therefore there is still an uncertainty on the window transmission of the instrument. Two sets of calibrated data are presented, one assuming a window transmission of 0.3 and a second one with a window transmission of 0.77. Care must be taken in the interpretation. Depending of the coefficient, the atmospheric opacity can become really low with some periods with 20-30 % of transmission. The calibration of window transmission will be determined during the summer campaign 2008-2009.

Using the Atmospheric transmission model of N. Schneider, it is possible to estimate the percentage of time for which there is a certain quantity of water vapour in the atmosphere. The result is given in Table 1.

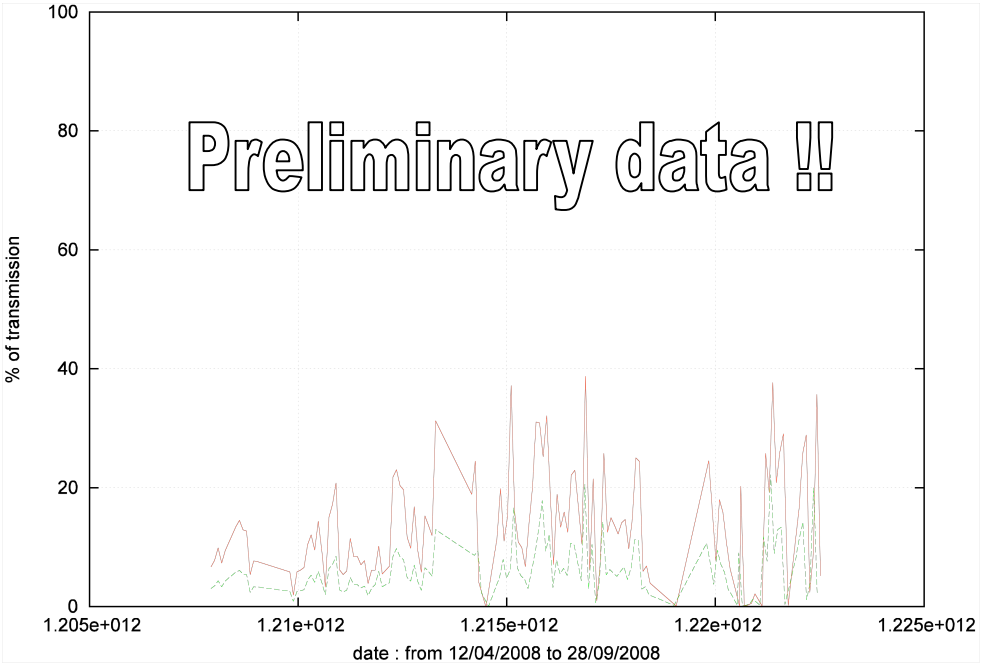

Figure 18: Transmission of the atmosphere at 200 µm at Dome C between April and September 2008, with a window transmission of 30% in red, a window transmission of 77% in green . The transmission is really good with some periods at 20-30 % for a window transmission of 30%.

	Window transmission 30%	Window transmission 77%
Pwv<0.1mm	3.2%	0%
Pwv<0.2mm	35%	1.2%
Pwv<0.3mm	69%	30%
Pwv>0.3mm	31%	70%

Table 1 : Percentage of time the atmosphere has a certain quantity of water vapour. The results are given in function of the window transmission.

2.5 Thermal gradients and effects of turbulence

2.5.1 Overall consideration

The thickness and intensity of the turbulent ground layer usually increase with wind speed. Since the Antarctic Plateau does not show significant topographic features, the energy content of the turbulent ground layer is directly related to the energy of the wind.

The stability of the Planetary Boundary Layer (PBL) can be evaluated from temperature vs. height profiles, from the heat flux and from SODAR measurements.

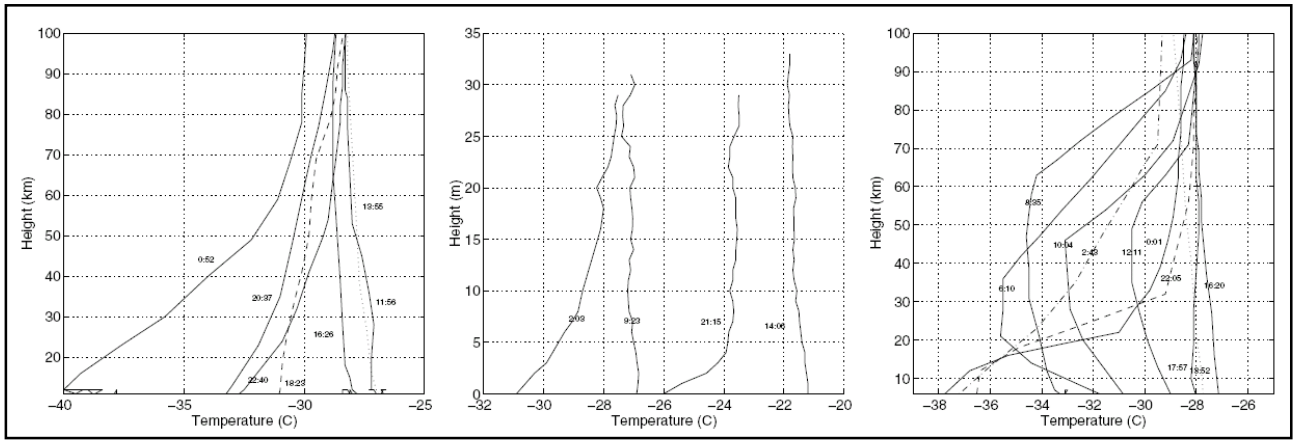

Figure 15: Left: temperature profiles taken at regular intervals on the 25/01/03; center: temperature profiles representative of the indicated hour measured using a pulley; right: temperature profiles taken at regular intervals on the 24/01/04.(From Aristidi et al.,2005)

The presence of a strong inversion layer in the first 20 m is evident between 8.00 and 17.00.

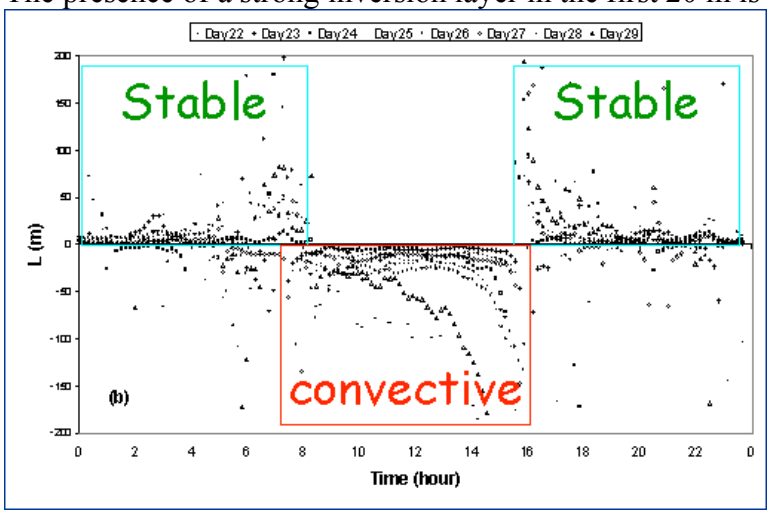

Figure 16: This figure report the Monin-Obhukov length measured in summer 1997. (Adapted from Georgiadis et al., 2002)

When the Monin-Obhukov length is negative, between approximately 8.00 and 17.00 LT, a convective activity is present. This is consistent with the PBL height measured by the SODAR measurements. However it is also reported in the same paper that the turbulence is extremely low and it is confined in the first 20m above the ground.

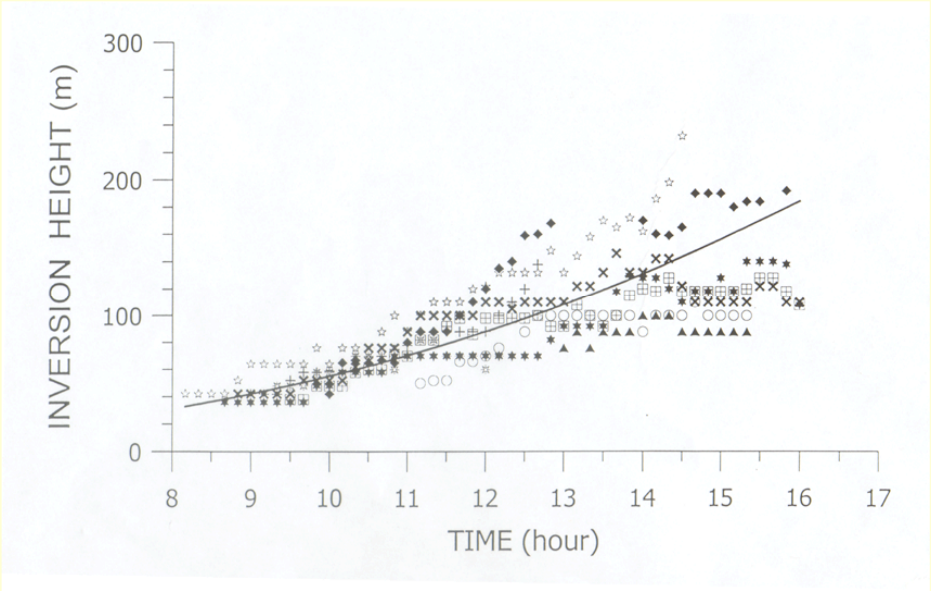

Thermal gradients

2.5.2 Thermal gradient and variabilities up to 46 m high

Common prerequisites for the design of unmanned telescopes at altitudes up to 46 m include the ongoing measurements of wind, humidity and temperature. The CEA team currently performs these measurements. The probes consist of 2 horizontal disks (CD like) distant by 10 mm to be used as sun shields. They are black inside, polished aluminium up and down. They are defrosted every 2 minutes for duration of 2 minutes. Inside is placed a thin aluminium cylinder (height 8mm, ø10mm) equipped with a Pt1000 small sensor and a small heater (0.25W) working together with disks heaters. The temperature sensor is red every 10 seconds continuously. Turbulence and air temperature stability might be derived afterward.

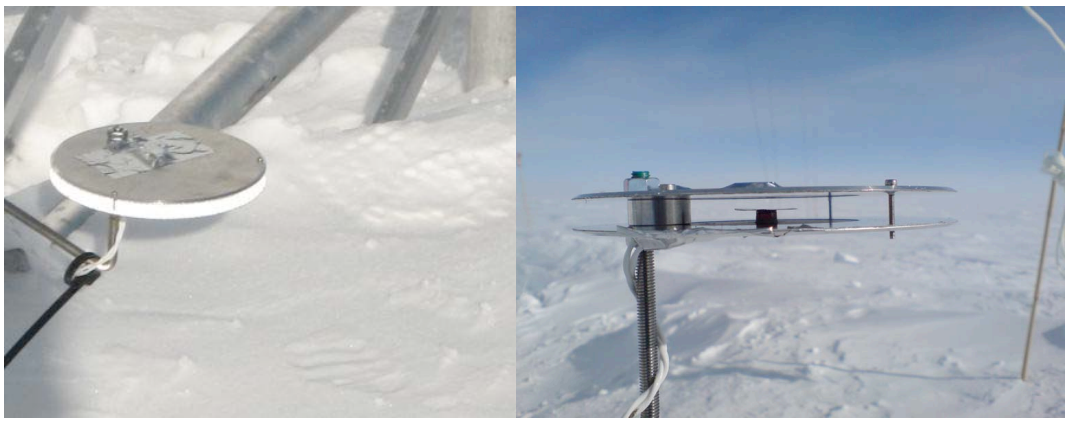

Figure 4: Left: Shielding of the thermal probes, the sunlight is back-reflected by the lower disk and forward reflected by the upper disk. Right : Pt1000 mounted on a ø20mm disk protected by ø150mm disks.

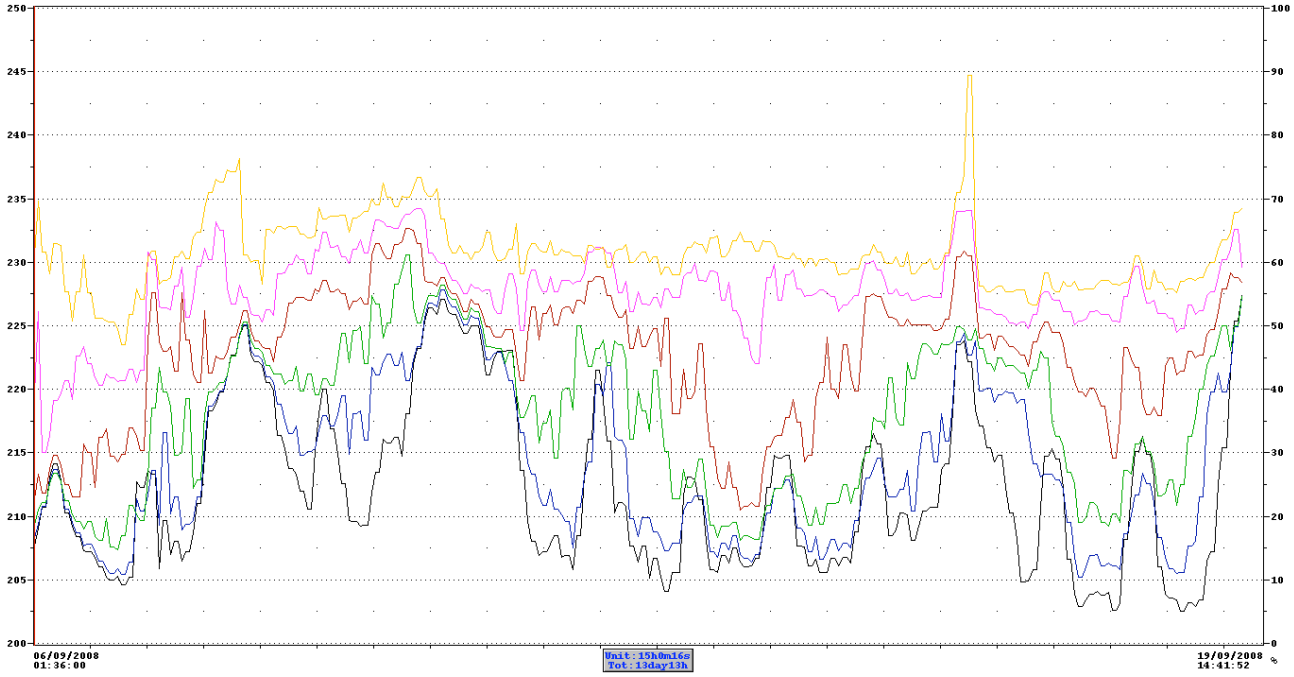

Figure 5: Temperatures in K measured at 0.2m, 2, 5, 12, 24 and 46m. Note that temperatures are lower at 0.2 m than at 46 m high. Variations of temperature with height go up to 20 K. Besides the temperature at 46m is rather stable compared to the temperature at 0.2m.

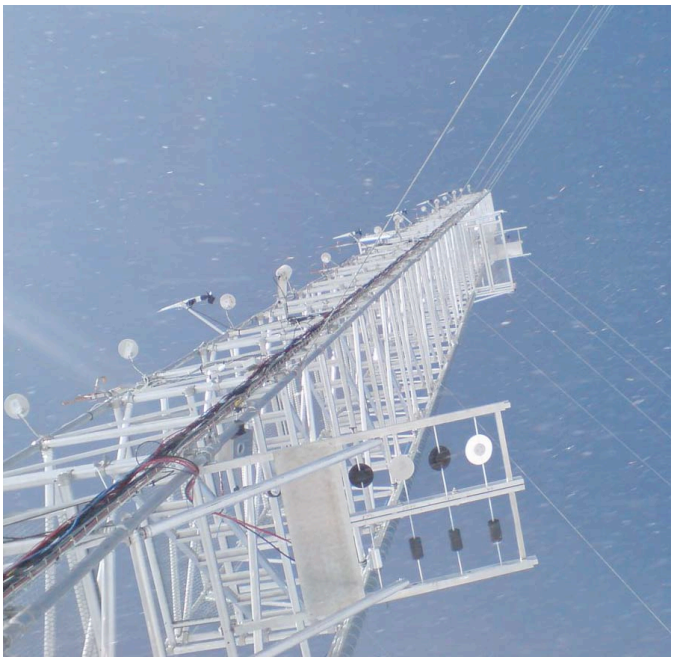

Figure 6: The temperature cells can be seen on the left of the tower. The frost cells are placed on two platform at 5m and 30m on the right of the 46m mast.

2.6 Frost formation

Dome C climate conditions severely impact and deform any telescope mirror and hardware. Whatever the telescope at Dome C the combination of little wind and high heat lost by radiation during the polar winter, results into a large thermal inversion and strong icing on all hardware objects. The CEA team currently tests different ways of protecting the instruments against frost.

16 temperature and wind measurements are performed from 0 to 46m, with closer altitude resolution near the ground. On an aluminium blade, we shall blow a 0.4x0.6 m^2 glossy aluminium

disk with fresh air blown from the ground in order to check if dry air may clean a surface in altitude (Figure 7).

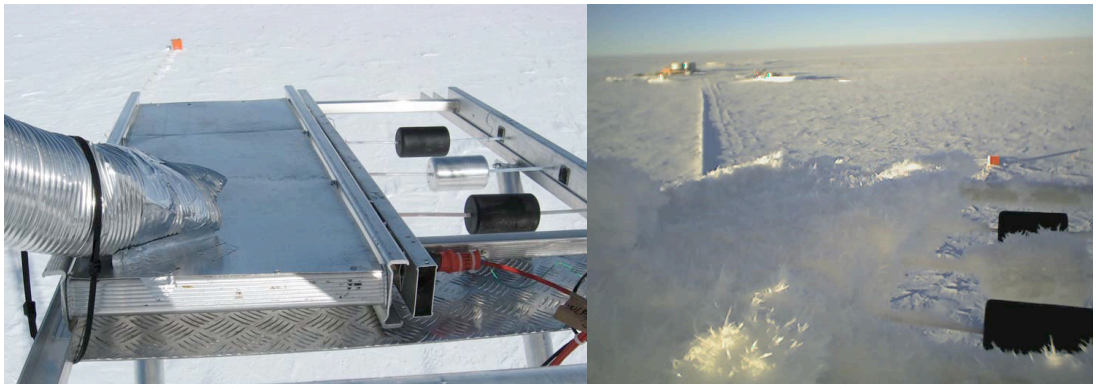

Figure 7: Left: At 30m a shiny aluminium surface is blowed with dry air from the ground level, near the 3 heated frost cells. Right: At 30m up to 6°C above ambient are sometimes needed to keep the cells clear of frost. The blower is not active on this photo. The crystals are typical frost built-up.

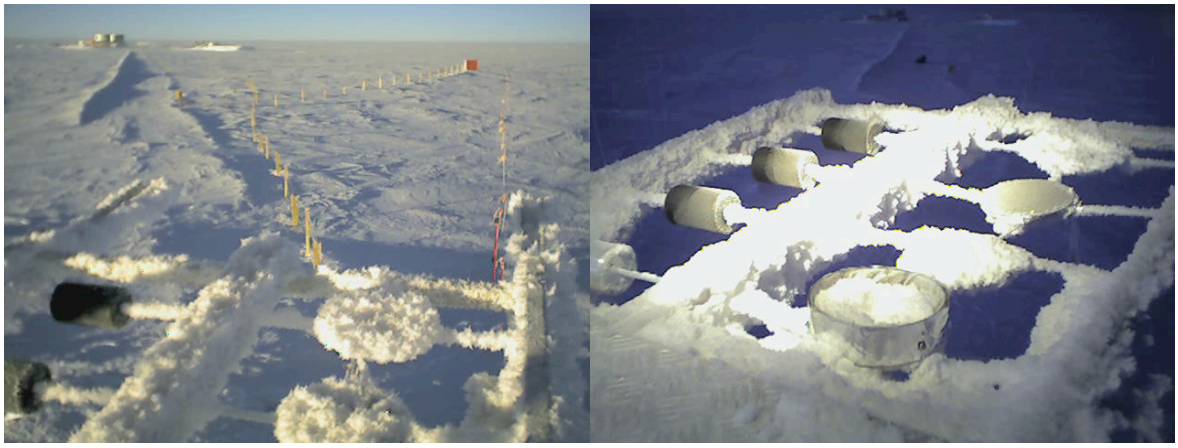

Figure 8: Left: On 17 april 2008, the frost has covered all the non-heated areas at 5m altitude. A heater at 3°C above ambient is needed to protect from frost built-up. Right: At 5m altitude a disk is surrounded by a heated ring to protect ice built-up on a simulated telescope. On this view the warming up of the ring T ambient + 3°C cannot stop the ice.

The COCHISE telescope (Roma 3 University) has been equipped by a system that will monitor the formation of frost on the telescope primary mirror and will try to stop its formation by heating for instance (Figure 9).

The measurements in process at Concordia will describe how much the air is super saturated at 5m and 30m. The strong temperature gradient blocks the air mixture. During 2007 winter campaign, the frost probes at 7m-altitude indicated super saturation of 75% above 100%. This is highly important as frost forms very quickly at Dome C on any piece of hardware. In the perspective of unmanned telescopes during polar winter, automatic removal of frost will be necessary for all type of telescope.

Figure 9: Left: The Italian 2.6m telescope Cochise equipped with infrared heaters, 24 holes to blow dry air and a heating system on the mirror. An efficient combination is a small warm up of the telescope to make the surface slippery in addition to blowers to flush the snow. Right: The infrared heaters remove the snow from the M2 support. This unprotected mirror accumulates frost toward the bottom. The M1 mirror in horizontal position is nearly clean. By tilting it, the snow would fall down.

Figure 10: Left: On this web-cam photo, the mirror is heated 5°C above ambient. The snow is pushed toward the centre of the mirror by both gravity and the blower. Right: Without a cleaning anti-frost system, the mirror is rapidly covered with frost and snow.

2.7 Atmospheric transmission modelling at Dome C and comparisons

2.7.1 MOLIERE

A versatile forward and inversion model for the millimetre and submillimetre wavelengths range, used in many aeronomy and some astronomy applications, is the MOLIERE code (Microwave Observation LIne Estimation and REtrieval). See Schneider et al. (2003) and Urban (2004) for its use for the analysis of ground-based and airborne microwave observations. MOLIERE has also been used for prediction/feasibility studies of future satellite projects for the exploration of the Earth and Mars atmospheres. A detailed mathematical description of the MOLIERE-5 forward and inversion model and the underlying principles is provided by Urban (2004). Designed for a variety of applications, the MOLIERE forward model comprises modules for spectroscopy, radiative transfer, and instrument characteristics. Important features of the absorption coefficient module are the line-by-line calculation as well as the implemented H2O, O2, N2, and CO2 continuum models (Borysow \& Frommhold 1986, Pardo 2001).

The radiative transfer module allows for calculations in different geometries such as limb and nadir sounding from orbiting platforms as well as up-looking observations of ground-based or airborne sensors. A spherically stratified (1-D) emitting and absorbing (non-scattering) atmosphere in local thermodynamical equilibrium is assumed, i.e. the source function is given by Planck's function.

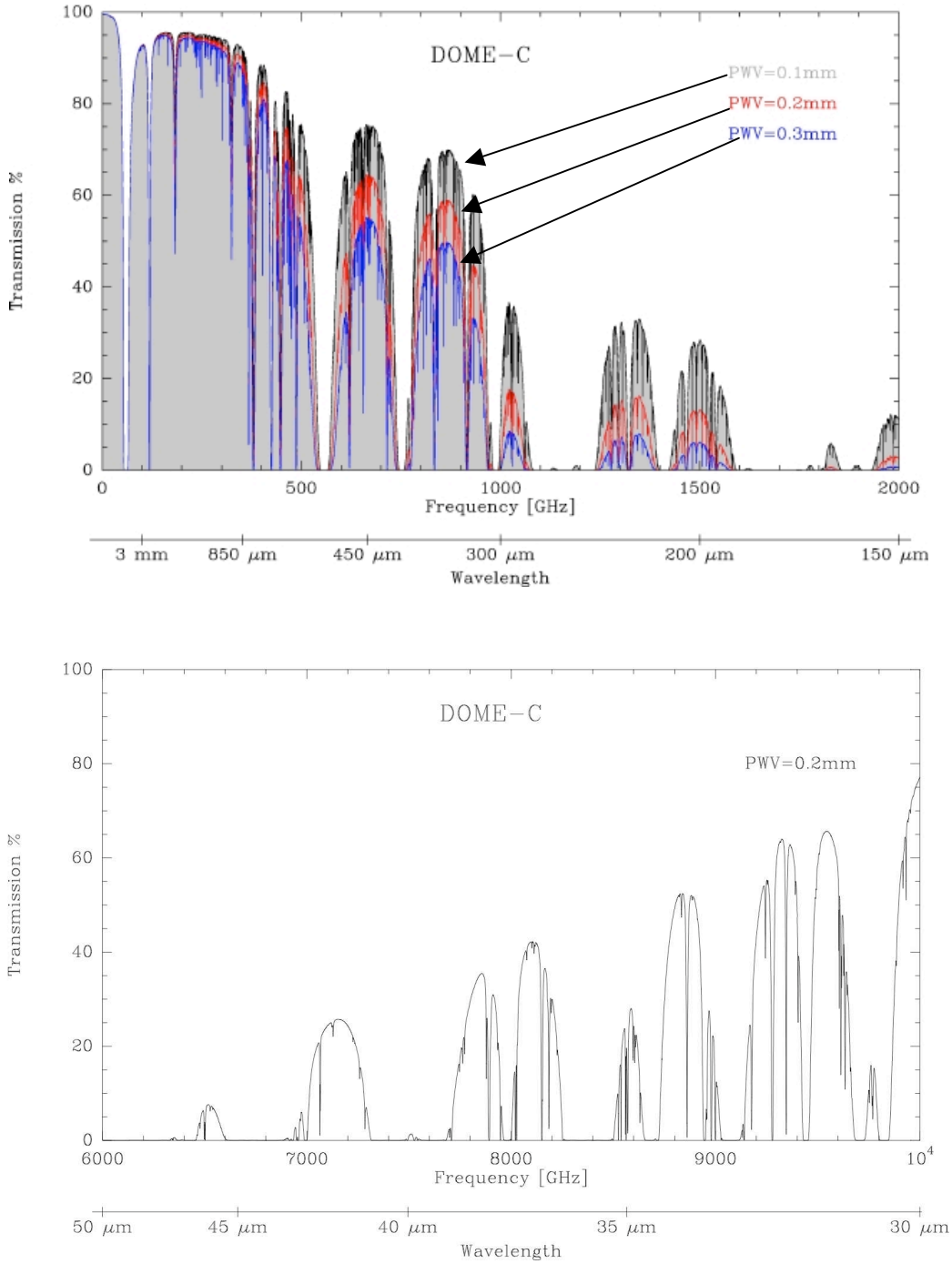

Figure 17: Modelled transmission for Dome C with the MOLIERE code. Transmissions were estimated using PWV=0.1, 0.2 and 0.3 mm in the submm/mm range (150 µm to 3 mm; upper figure) and PWV=0.2 mm for the far-infrared range (lower figure). Many observing windows open between 30 and 50 µm. The 200 µm (1500 GHz) windows opens at Dome C under PWV<0.5 mm. Note: MOLIERE (Microwave Observation LIne Estimation and REtrieval) is a versatile forward and inversion model for the millimetre and submillimetre wavelengths range, used in many aeronomy and some astronomy applications (Urban 2004).

The geometrical radiation path is corrected for the effect of refraction. Weighting functions, required for inversions, are calculated by differentiating the radiative transfer equation analytically after discretisation. The radiative transfer model is supplemented by a sensitivity module for estimating the contribution to the spectrum of each catalogue line at its centre frequency, enabling the model to effectively filter large spectral data bases for relevant spectral lines. Several

independent modules permit accurate simulation of instrument characteristics such as the antenna field-of-view, the sideband response of a heterodyne receiver, as well as the spectrometer bandwidth and resolution. Frequency switched observations may also be modelled.

We use temperature- and pressure profiles from the ODIN satellite (zonal mean over 10 degrees) and the U.S. standard H2O profile for 45N. To produce to the different pwv-values (considering the altitude of the site), we simply scale the tropospheric part of the U.S. standard profile accordingly. The spectral line catalog was compiled from the HITRAN and JPL data bases and covers the frequency range 0-10 THz.

Atmosperic models for DOME C were calculated for pwv values of 0.1, 0.2, and 0.3 mm (see Fig. xxx). The transmission curves show several atmospheric windows in the FIR that open around, e.g., 150, 200, 220, 350 and 450 microns. At a pwv of 0.1 mm, the transmission is 30% at 200 µm and thus comparable to the value of 40% (Fig. yyy) for the higher altitude site of CCAT (Cornell Caltech Atacama Telescope in Chile).

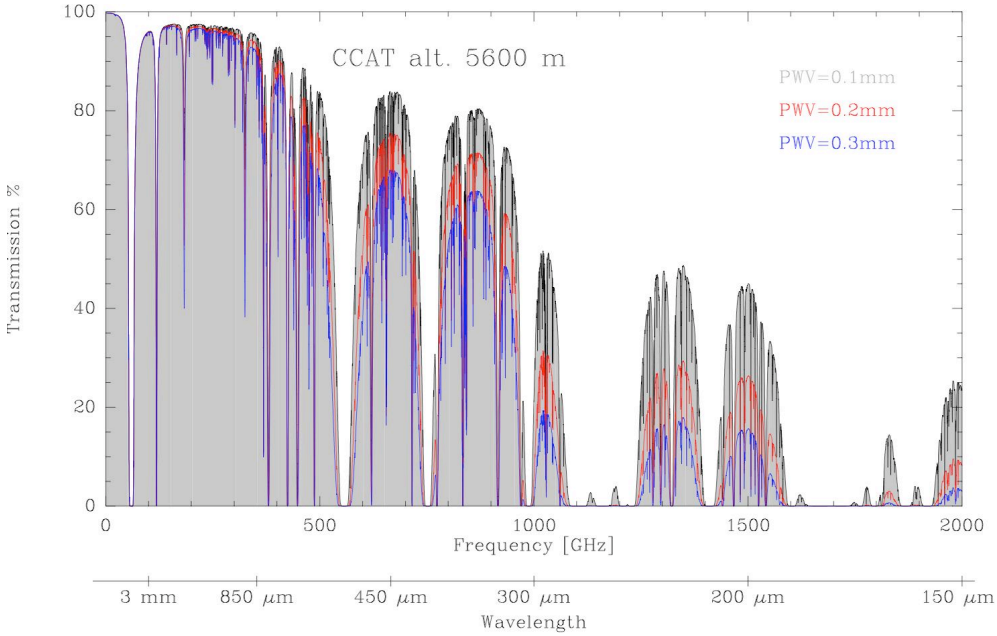

Figure 2: Modelled transmission for the CCAT site on Cerro Chajnantor with the MOLIERE code. Transmissions were estimated using PWV=0.1, 0.2 and 0.3 mm in the submm/mm range.

2.7.2 ATM

A comparison between Dome C and South Pole stations, based only on synthetic spectra as derived by ATM code assuming average values for the atmospheric ground parameters, points out a low dry continuum and H_2O pseudocontinuum contributions at Dome C resulting it in a low total opacity, especially in the THz spectral range. The reason of this behaviour is mainly due to a lower pressure at Dome C while the minimum ground temperatures are almost the same in both the stations.

In order to continuously monitor the atmospheric transmission several approaches are possible: tippers or tau-meters, hygrometers, water vapour radiometers, radiosounding data and spectrometers.
We want to highlight that only by spectra, all over the interested spectral range, it is possible a precise monitoring of the total opacity at each frequency at the price of a bit complex instrument. In fact the first approaches allow a continuous recording of data by simple instruments but with the drawback of single frequency observations needing a synthetic atmospheric model for inferring the transmission at different frequencies.

We suggest to dedicate for Dome C a spectrometer in the submm/mm range for continuous observations. In the meantime we have produced estimates of atmospheric transmission using available radiosounding data.

We have analysed data recorded by radiosoundings (atmospheric temperature, relative humidity and pressure vs altitude) at Dome C.The data have been corrected by possible systematics and, using the ATM code, atmospheric emission profiles have been produced. In this way we have established about 470 synthesized atmospheric spectra in the region between 100 GHz 41 THz from May 2005 until January 2007, one or two times for day (see De Gregori S. et al. in preparation).

The first step of the analysis was to recover pwv values for the whole period. Two main features are evident from the data: low values of pwv (less than 0.5mm during autumn months) unfortunately with a large dispersion (50% or more), i.e. low stability.
In order to produce a more quantitative analysis we have considered several photometric bands having astrophysical and cosmological involvements. The bands are centred around f_p with realistic bandwidths BW (i.e. bandwidths similar to existing experiments) The values are the following: f_p150 GHz- BW 10%, f_p210 GHz- BW 7%, f_p270 GHz- BW 5%, f_p360 GHz- BW 4%, f_p660 GHz- BW 16%, f_p870 GHz- BW 12%, f_p1500 GHz- BW 7%.
Checking monthly averages and relative dispersions of in band transmissions the results are not encouraging. Apparently there is not a common favourable period for all the bands and dramatic fluctuations are present in the THz windows.

Two outcomes can be gathered from this analysis. If we believe in the transmission values, as deduced by radiosounding data, in order to control the low stability we need a continuous and more frequent atmospheric sampling. In the case that we consider the radiosounding data not accurate enough for estimating by model atmospheric properties we need other observational approaches.

2.8 Future plans

2.8.1 CAMISTIC: 200 μm bolometer array

The CAMISTIC project aims to install a filled bolometer-array camera with 16x16 pixels on a small telescope, possibly the IRAIT telescope (Tosti et al. 2006), at Dome C. CAMISTIC will explore the 200-μm (i.e. THz) windows for ground-based observations. CAMISTIC will perform site testing on the atmospheric transmission and sky noise in the 200-μm range. Sky noise measurements will be performed through sky imaging with the whole bolometer array. On a 80-cm telescope (IRAIT), the near field is located at 1.6 km for 200 μm. This means that the overlap between the bolometer pixel beams will be greater than 50% until about 1 km, and above the near-field limit, the pixel beams completely diverge. If the water vapour cells responsible for the fluctuations in the atmosphere background power (i.e. sky noise) are located below about 1 km, the pixels "see" through the same atmosphere column and sky noise. However, if these water vapour cells are above 1.6 km, then non adjacent pixels on the array "see" through different atmosphere column and can potentially provide a map of the sky noise.

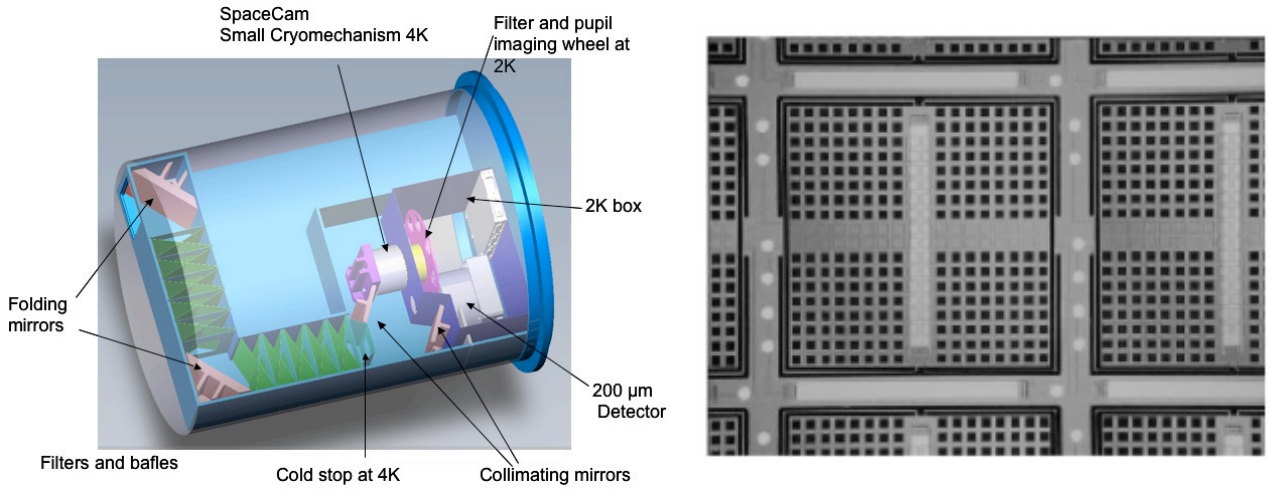

Figure 8: Left: View of the cryostat and optics to be installed on IRAIT in 2010. Right: View on a bolometer pixel of a 256-pixel bolometer unit similar to the ArTéMiS and PACS bolometer units (Talvard et al, SPIE conference 7020).

2.8.2 CASPER: Martin-Puplett interferometer

Few years ago we have proposed to PNRA, but we are still waiting for an answer, a spectrometer devoted to measurements of atmospheric emission between 3455 cm^{-1} at Dome C. CASPER (Concordia Atmospheric SPectroscopy of Emitted Radiation) will produce atmospheric spectra with a 1% precision, at different zenithal angle with an angular scale in the sky of the order of 30' with a spectral resolution less then 0.2 cm^{-1}.
CASPER is specifically devoted to characterize the site for future FIR/mm telescope. Atmospheric data recorded by CASPER will allow for correction of astrophysical and cosmological observations without the need for telescope-specific procedures and further loss of observation time (i.e. skydips). In fact calibration of ground based telescopes by known sky sources observations is strongly affected by atmospheric absorption. CASPER has this as its primary goal.
The knowledge, in real time, of atmospheric radiation in a large spectral range allows an accurate estimate of the opacity and the precipitable water vapour values.
CASPER is based on a Martin-Puplett interferometer with two inputs (sky signal and reference source) and two outputs. The instrument can perform two techniques for recording data: a fast scan acquisition (mainly for spectrometric measurements of the atmosphere) and a phase modulation (specifically for very low S/N ratios like for measurements of the polarized component of the sky brightness). The sky radiation is collected into the interferometer through a Pressman-Camichel 62-cm in diameter telescope with a field of view equals to 1 degree and having the possibility to explore the full range of zenithal angles.
The whole frequency range is splitted into two bands (Low Frequency Band: 3415 cm^{-1} and High Frequency Band: 20455 cm^{-1}) for removing the excess of radiative background on the distinct couples of bolometric detectors cooled at 300 mK and 4 K respectively.
A prototype version of CASPER has been developed for MITO (Millimeter and Infrared Testagrigia Observatory, 3500 m a.s.l. – Val d'Aosta - Italy) with a limited spectral range 3412 cm^{-1}.

2.9 Conclusions

Comparison with other sites
The comparison with other relevant sites is reported in table XX.

TABLE 2 – Comparison among the mean values of precipitable water *W* and the corresponding quartile values found from the present Dome C data-sets, the Dome C data-sets of Valenziano and Dall'Oglio (1999) (referred to as VD data), and the South Pole findings of Chamberlin (1997) relative to the austral winter and summer periods.

Measurement site	Measurement period	Values of precipitable water *W* (mm STP)			
		Mean	1st quartile	Median	3rd quartile
Dome C (winter 2008)	March-now	To	be	calibrated	
Dome C (present results)	December-January, 2003/2004	0.76 ± 0.20	0.60	0.71	0.90
Dome C (present results)	March-April-May, 2005	0.28 ± 0.09	0.22	0.25	0.34
South Pole (Chamberlin et al., 1997)	Austral Winter, 1995	-	0.19	0.25	0.32
South Pole (Chamberlin et al., 1997)	Austral Summer, 1995/96	-	0.43	0.54	0.72
Mauna Kea (Hogg, 1992)	January – June, WWWW	-	1.05	1.65	3.15
Mauna Kea (Hogg, 1992)	July – December, YYYY	-	1.73	2.98	5.88
Atacama (Lane, 1998)	April – September, 1995		0.68	1.00	1.60
Atacama (Lane, 1998)	October – March, 1995/96		1.10	2.00	3.70
Atacama (Giovanelli et al., 2001) 5000 m altitude	October 1998 – August 2000		0.71	1.04	1.75

2.10 Bibliography

Aristidi, E., A. Agabi, J. Vernin, M. Azouit, F. Martin, A. Ziad, and E. Fossat (2003), Antarctic site testing: First daytime seeing monitoring at Dome C, Astron. & Astrophys., 406, L19-L22.

Aristidi, E., K. Agabi, M. Azouit, E. Fossat, J. Vernin, T. Travouillon, J. S. Lawrence, C. Meyer, J. W. V. Storey, B. Halter, W. L. Roth, and V. Walden (2005), An analysis of temperatures and wind speeds above Dome C, Antarctica, Astron. & Astrophys., 430, 739-746.

Aristidi, E., Agabi, A., Azouit, M., Fossat, E., Vernin, J., Sadibekova, T., Travouillon, T., Lawrence, J. S., Halter, B., Roth, W. L., and Walden, V. P. 2005. Site testing study based on weather balloons measurements, EAS 14, 227

Aristidi, E., Agabi, A., Fossat, E., Azouit, M., Martin, F., Sadibekova, T., Travouillon, T., Vernin, J., and Ziad, A. 2005. Site testing in summer at Dome C, Antarctica, A&A 444, 651

Aristidi, E., Agabi, A., Fossat, E., Azouit, M., Vernin, J., Sadibekova, T., Travouillon, T., Ziad, A., and Martin, F. 2005. Site testing in winter at Dome C, sf2a.conf 45

Aristidi, E., Agabi, A., Fossat, E., Travouillon, T., Azouit, M., Vernin, J., Ziad, A., Martin, F., and Robuchon, G. 2005. Daytime site testing at Dome C: Results of 2003 2004 campaign, EAS 14, 13

Beaupuits Juan Pablo Pérez, Otárola Angel, Rantakyrö Fredrik T., Rivera Roberto C., Radford Simon J.E., Nyman Lars-Åke 2004, Analysis Of Wind Data Gathered At Chajnantor, ALMA Memo no. 497

Bally, J. (1989), Atmospheric transparency over Antarctica from the mid-infrared to centimeter wavelengths, in Astrophysics in Antarctica, edited by D .J. Mullan, M. A. Pomerantz, and T. Stanev, AIP Press, New York, pp. 100 - 105.
Bolton, D. (1980), The computation of equivalent potential temperature, Mon. Wea. Rev., 118, 1046-1053.
Calisse, P. G., M. C. B. Ashley, M. G. Burton, M. A. Phillips, J. W. V. Storey, S. J. E. Radford, and J. B. Peterson (2004), Submillimeter site testing at Dome C, Antarctica, Publ. Astron. Soc. Aust., 21, 1-18.

Calisse, P. G., Ashley, M. C. B., Burton, M. G., Lawrence, J. S., Travouillon, T., Peterson, J. B., Phillips, M. A., Radford, S. J. E., and Storey, J. W. V. 2004. Dome C, Antarctica: The Best Accessible Sub-millimetre Site on the Planet?, dimg.conf 353

Lane, A.P. (1998), Submillimeter transmission at South Pole, Astrophysics from Antarctica, ASP Conf. Series, 141, 289-295.

Lawrence, J. S., M. C. B. Ashley, A. Tokovinin, and T. Travouillon (2004), Exceptional astronomical seeing conditions above Dome C in Antarctica, Nature, 431, 278-281.

Mould, J. R., Mighell, K., Merrill, M., Lynds, R., Tokovinin, A., Travouillon, T., Moore, A., Pennypacker, C., Wang, L., Weidner, G., Swain, M., and York, D. 2006. Astronomical Site Testing of the Antarctic Plateau, IAUSS 7,

Georgiadis, T., et al., 2002, Boundary layer convective-like activity at Dome Concordia, Antarctica, Nuovo Cimento C Geophysics Space Physics C, 25, 425

Luers, J. K. and Eskridge, R. E. 1995. Temperature Corrections for the VIZ and Vaisala Radiosondes., JApMe 34, 1241

Miloshevic, L. M., A. Paukkunen, H. Vömel, and S. J. Oltmans (2004), Development and validation of a time-lag correction for Vaisala radiosonde humidity measurements, Jour. Atmos. Oc. Techn., 21, 1305-1327.

Miloshevich, L. M., Vömel, H., Whiteman, D. N., Lesht, B. M., Schmidlin, F. J., and Russo, F. 2006. Absolute accuracy of water vapor measurements from six operational radiosonde types launched during AWEX-G and implications for AIRS validation, JGRD 111, 9

Tomasi, C., A. Cacciari, V. Vitale, A. Lupi, C. Lanconelli, A. Pellegrini, and P. Grigioni (2004), Mean vertical profiles of temperature and absolute humidity from a twelve-year radiosounding data-set at Terra Nova Bay (Antarctica), Atmos. Res., 71, 139– 169.

Tomasi, C., Petkov, B., Benedetti, E., Vitale, V., Pellegrini, A., Dargaud, G., De Silvestri, L., Grigioni, P., Fossat, E., Roth, W. L., and Valenziano, L. 2006. Characterization of the atmospheric temperature and moisture conditions above Dome C (Antarctica) during austral summer and fall months, JGRD 111, 20305

Tomasi, C., Petkov, B., Benedetti, E., Valenziano, L., Lupi, A., Vitale, V., and Bonafé, U. 2008. A Refined Calibration Procedure of Two-Channel Sun Photometers to Measure Atmospheric Precipitable Water at Various Antarctic Sites, JAtOT 25, 213

Travouillon, T. 2005. Seasonal variations of the boundary layer turbulence at Dome C, EAS 14, 31

Valenziano, L., et al. (1998), APACHE96. CMBR anisotropy experiment at Dome C, in Astrophysics From Antarctica, edited by G. Novak and R. H. Landsberg, pp. 81– 89, Astron. Soc. of the Pac., San Francisco, Calif.

Valenziano, L., and G. Dall'Oglio (1999), Millimetre astronomy from the high Antarctic Plateau: site testing at Dome C, Publ. Astron. Soc. Aust., 16, 167-174.

Valenziano, L. 2005. Astronomical site quality in the sub-millimetric and millimetric bands at Dome C, Antarctica, EAS 14, 25

Volz, F. E. 1983. Comments on `Precipitable Water Measurements with sun Photometers'., JApMe 22, 1967

Wang, J., Cole, H. L., Carlson, D. J., Miller, E. R., Beierle, K., Paukkunen, A., and Laine, T. K. 2002. Corrections of Humidity Measurement Errors from the Vaisala RS80 Radiosonde: Application to TOGA COARE Data, JAtOT 19, 981

Borysow, A., Frommhold, L., 1986, ApJ 311, 1043

Pardo, J., Cernicharo, J., Serabyn, E., 2001, I3ETAP 49 (12), 1683

Schneider, N., Lezeaux, O., de La N\"oe, J., Urban, J., Ricaud, P., JGR, 108, D17, 4540, 2003.

Urban, J., Baron, P., Lauti\'e, N., Schneider, N., et al., J. Quant. Spectros. Radiat. Transfer 83, 529, 2004.